



**HAL**  
open science

## From macroplastics to microplastics: Role of water in the fragmentation of polyethylene

Fanon Julienne, N. Delorme, Fabienne Lagarde

### ► To cite this version:

Fanon Julienne, N. Delorme, Fabienne Lagarde. From macroplastics to microplastics: Role of water in the fragmentation of polyethylene. *Chemosphere*, 2019, 236, pp.124409. 10.1016/j.chemosphere.2019.124409 . hal-02318540

**HAL Id: hal-02318540**

**<https://hal.science/hal-02318540>**

Submitted on 25 Oct 2021

**HAL** is a multi-disciplinary open access archive for the deposit and dissemination of scientific research documents, whether they are published or not. The documents may come from teaching and research institutions in France or abroad, or from public or private research centers.

L'archive ouverte pluridisciplinaire **HAL**, est destinée au dépôt et à la diffusion de documents scientifiques de niveau recherche, publiés ou non, émanant des établissements d'enseignement et de recherche français ou étrangers, des laboratoires publics ou privés.



Distributed under a Creative Commons Attribution - NonCommercial 4.0 International License

# 1 From macroplastics to microplastics: 2 role of water in the fragmentation of polyethylene

3  
4 Fanon Julienne<sup>1</sup>, Nicolas Delorme<sup>1</sup>, Fabienne Lagarde<sup>1\*</sup>

5  
6 <sup>1</sup>*Le Mans Université, Institute of Molecules and Materials of Le Mans – IMMM-UMR-CNRS*  
7 *6283, 72085 Le Mans Cedex 9, France*

8  
9 \*corresponding author: Dr Fabienne LAGARDE, Le Mans Université, Institute of Molecules  
10 and Materials of Le Mans – IMMM-UMR-CNRS 6283, 72085 Le Mans Cedex 9, France. Tel:  
11 +33 263833267 - fabienne.lagarde@univ-lemans.fr

## 12 **Abstract**

13 In this work, the artificial photodegradation of polyethylene films was studied in laboratory to  
14 compare the fragmentation pathways of this polymer at air and in water. Oxidation, surface  
15 mechanical properties, crystallinity and crack propagation were monitored to investigate their  
16 influence on fragmentation. Without any external stress, fragmentation only occurred in water  
17 despite a higher level of oxidation for films weathered at air. The cracking of the films did not  
18 appear correlated with the oxidation level and the presence of water appeared as a promoter of  
19 cracking propagation. The results also showed that the mechanical properties at the surface  
20 play a major role in the fragmentation pathway whereas the fabrication process may influence  
21 the propagation direction of the cracks. Consequently, the distribution in size of plastic  
22 fragments in the aquatic environment may be linked to the nature of the polymer but also to  
23 its manufacturing process. In this study, after 25 weeks of weathering in water, 90 % of the  
24 fragments were > 1 mm with very similar shapes showing that micrometric fragments were

25 not yet abundant. These results suggest that long times of weathering in water and many steps  
26 of fragmentation appear necessary from macroplastics to reach sizes < 1 mm in the aquatic  
27 environment. These results constitute a first attempt to understand the pathways leading from  
28 macroplastics to microplastics in water. They have to be confirmed for other polymers and the  
29 long-term behavior of the fragments needs to be studied to predict their decrease in size  
30 among time.

31

32 **Keywords:** microplastics; macroplastics; fragmentation; polyethylene; weathering;  
33 photodegradation.

34

35

## 36 **Introduction**

37 After 60 years of industrial life, plastics have become omnipresent in our lives but their end of  
38 use raises concern. It was approximated that in the last 50 years, 12,000 Mt of plastics  
39 escaped from the waste management cycle and entered in landfills or directly in the  
40 environment (Geyer, Jambeck, and Law 2017). Once in the aquatic environment, macro  
41 debris of plastic undergo mechanical (erosion, abrasion), chemical (photo-oxidation,  
42 hydrolysis) and biological (degradation by microorganisms) modifications (Andrady 2017).  
43 All these actions lead to the weathering and the fragmentation of plastic macro debris in  
44 smaller and more abundant pieces called microplastics when their size is under 5 mm (Arthur,  
45 Baker, and Bamford 2009). Theoretically, the final degradation of a polymer would be  
46 reached when it is mineralized. The amount of time for a complete degradation of inert plastic  
47 polymers such as PE or PP in the marine environment is roughly estimated to several  
48 hundreds of years and this degradation is probably the results of several complex processes  
49 with various kinetics (Barnes et al. 2009; Gewert, Plassmann, and MacLeod 2015). It is

50 particularly difficult to monitor all these processes in the real environment and laboratory  
51 studies are still necessary to obtain more accurate data and to identify the pathways leading to  
52 an eventual bio-assimilation of plastic debris in the aquatic environment. Among all  
53 processes, the abiotic degradation of polymers in the environment leading to their  
54 fragmentation is of particular interest. Indeed, a lot of studies aimed to study the loss of  
55 mechanical properties in polymer during their ageing but experimental studies on their  
56 fragmentation at air or in water are scarce (Jahnke et al. 2017; Kalogerakis et al. 2017) and the  
57 ultimate size distribution of polymer fragments that can be generated during environmental  
58 fragmentation is not really known raising the question of the possible presence of great  
59 quantities of nanoplastics in the future (Koelmans et al. 2017).

60 The parameters that can modify the fragmentation pathways (polymer nature or structure,  
61 environmental conditions) are not totally identified and it is important to verify if some of  
62 these parameters can impact the ultimate size of generated fragments. However, monitoring  
63 fragmentation in real environment is quite impossible due to the potential loss of generated  
64 fragments. In this study, the long-term artificial weathering of polyethylene films was studied  
65 in laboratory in order to monitor the first stages of the fragmentation under two different  
66 environments: in air or in Milli-Q water. Since this work is a first study to provide  
67 understanding of the fragmentation pathways and kinetics, models as simple as possible were  
68 selected in order to identify to what extent each parameter (water vs air) impact separately the  
69 processes at stake. Polyethylene was chosen as it is the polymer the most commonly found in  
70 the environment (Phuong et al. 2016). Fragments are supposed to be generated when cracking  
71 lines converge. The key to predict the fragment number and size is then to study the  
72 appearance and behavior of cracks in the material. Crack propagation inside a material  
73 follows two principal modes differing by their speed of propagation, either named rapid crack  
74 propagation (RCP) or slow crack growth (SCG) (Alkhadra et al. 2017; Šindelář et al. 2005).

75 SGC mechanism has been widely studied in polymers, these fractures are characterized by the  
76 stable growth of a crack with little deformation in the plastic material. RCP has been mainly  
77 studied in mineral material but it has been also observed for HDPE pipes in contact with  
78 pressurized gas or chlorine solution (Choi et al. 2009; Frank, Pinter, and Lang 2009). The  
79 fragmentation mechanism is not completely elucidated for semi-crystalline polymers,  
80 especially in water, but observation seems to indicate that cracks are initiated on an impact  
81 event and can travel long distances rather quick. The aim of this work is to provide  
82 information on the link between oxidation, cracks formation and size of fragments in  
83 polyethylene films under weathering and to investigate the role of water in these processes.

84

85

## 86 **Experimental part**

87

### 88 *LDPE films*

89 Low density Polyethylene (LDPE) films (2x2cm) with the same thickness (i.e. 24(3)  $\mu\text{m}$  as  
90 measured by micrometer) and the same roughness (i.e. 25(5) nm as measured by AFM on  
91 30x30 $\mu\text{m}^2$  image) were selected from a film obtained by a blown-extrusion process. To avoid  
92 external mechanical stress which can promote fragmentation sample manipulation was as  
93 limited as possible. The films were cut to make a distinction between the top face (toward the  
94 lamp) and the bottom face (toward the beaker). The manufactured pellets (Alcudia PE-003)  
95 were provided with the mention: «does not contain any additives» and no additives could be  
96 detected by Infrared and Raman spectroscopies. As determined by Differential Scanning  
97 Calorimetry, LDPE films have a melting point of 112°C and a degree of crystallinity of 32%.  
98 This partial level of crystallization corresponds to a semi-crystalline polymer.

99

100 *Accelerated weathering conditions*

101 Two environments conditions were modeled. Films were placed either in empty quartz  
102 beakers for air condition (directly in contact with the bottom of the beaker.) or beakers filled  
103 with MilliQ water without stirring (water condition). It has to be noted that since LDPE is less  
104 dense than water, films are floating on the surface of the water. For each condition, two  
105 replicates that were never manipulated until the fragmentation were characterized.

106 To reproduce the sunlight exposure, each sample was placed in a XLS+ chamber equipped  
107 with a xenon lamp. The ageing conditions were fixed to correspond to the ISO 4892-3:2013  
108 standard. The irradiation intensity was around 60 W/m<sup>2</sup> which correspond to a total amount of  
109 solar radiation 9x10<sup>9</sup> J/m<sup>2</sup>, and a temperature between 32-44°C.

110

111

112 *Characterization of fragments*

113 FTIR spectra were acquired using a Fourier transform infrared microscopy system (μFT-IR;  
114 Spotlight 200i FT-IR microscopy system, PerkinElmer) in transmission mode as the thickness  
115 of the samples was small enough to avoid saturation, therefore spectra and indices take into  
116 account both sides of the film and its volume. For each film, three measurements were done  
117 randomly on the film using the microscope with an aperture of 100 x 100 μm. Measurements  
118 were realized with 32 accumulations ranging from 4000 to 600 cm<sup>-1</sup>. The spectra were then  
119 baseline corrected with the software “Spectrum”.

120 To evaluate the oxidation of PE, three oxidative indexes were calculated as the ratios of

121 integrated intensities for different wavelength as follows  $CI = \frac{I_{1970-1560}}{I_{1450-1540}}$ ,  $HI = \frac{I_{3900-3200}}{I_{1450-1540}}$  and

122  $VI = \frac{I_{940-885}}{I_{1450-1540}}$ .

123

124 Raman spectroscopic measurements were conducted using a confocal laser Raman  
125 spectrometer (Xplora, Horiba). The Raman signals were recorded in a spectral range 600 to  
126  $3500\text{ cm}^{-1}$  with an integration time of 30 s using a 638 nm laser excitation wavelength in  
127 combination with a  $\times 50$  objective of an Olympus BX41 microscope. Raman analysis, were  
128 only performed once the films were fragmented into small pieces and it was not possible to  
129 guarantee which face was under investigation. Accordingly, the measurements were  
130 performed on several fragments and then averaged. All the raw data were then treated with  
131 Lab Spec 5 software for linear baseline correction, and Peakfit software for the smoothing  
132 and the peaks deconvolution. The crystallinity was calculated as  $1 - \frac{I_{1303}}{I_{1292}}$ .

133

134 Atomic Force Microscopy (Agilent 5500AFM) was used. Surface topography was measured  
135 in ambient condition using tapping mode with tip (calculated tip stiffness=5N/m). Force-  
136 volume measurements (100 curves/sample) were performed in contact mode (calculated tip  
137 stiffness=43N/m). Measurements of the elastic properties of the weathered films were  
138 conducted following the procedure developed by Oliver and Pharr (Schiffmann 2011).

139

#### 140 *Fragment Size Distribution*

141 After 25 week of aging the PE film appeared fragmented in water. The vial containing the PE  
142 fragments was placed between a polarizer and a circular analyzer to take a photograph in  
143 polarized light. The device can image objects down to a size of  $50\text{ }\mu\text{m}$ , below which the  
144 contours become blurred, so no conclusion could therefore be drawn on the part of the  
145 distribution below this size. The images were processed using the Gwyddion software, giving  
146 access to the numbers, sizes and positions of the objects. The longest size of each fragment  
147 was measured, ranked and the distribution could be traced.

148

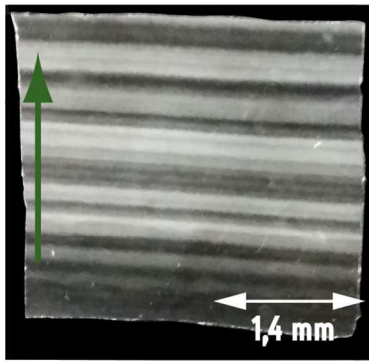
149 **Results**

150 ***Fragmentation***

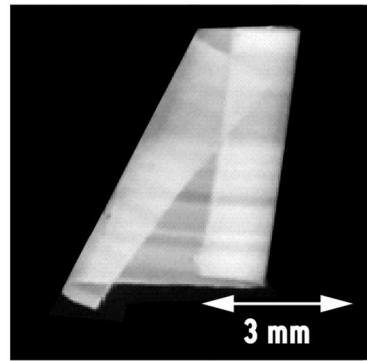
151 As shown by Figure 1, between crossed polarizer, lines parallel to the film extrusion direction  
152 can be observed on the as prepared (pristine) LDPE film. These lines originate from the  
153 induced stress brought by the process of film formation (passage through the extrusion die  
154 and fast coldening) (Zhang et al. 2004). After 25 weeks of accelerated weathering with no  
155 manipulation, the replicates in water have fragmented in anisotropic bended fragments with  
156 the longer length in a normal direction toward the extrusion direction. The size of the  
157 fragments appeared as a large distribution from 0.4 to 7 mm in length with 62 % on average  
158 of the fragments which correspond to the definition of microplastics (< 5 mm). After the same  
159 weathering time in air, the films were not fragmented but appeared coiled upon themselves  
160 along the extrusion direction. These first observations indicate clearly that the environment  
161 influences the fragmentation pathways of LDPE films.

162

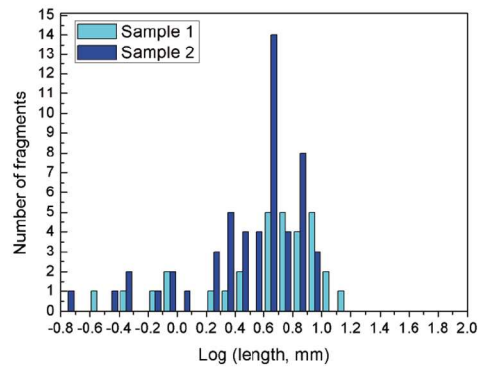
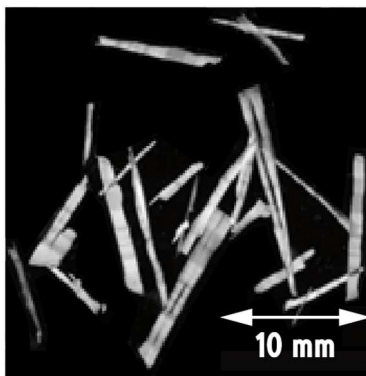
Pristine film



Weathered in air



Weathered in water



163

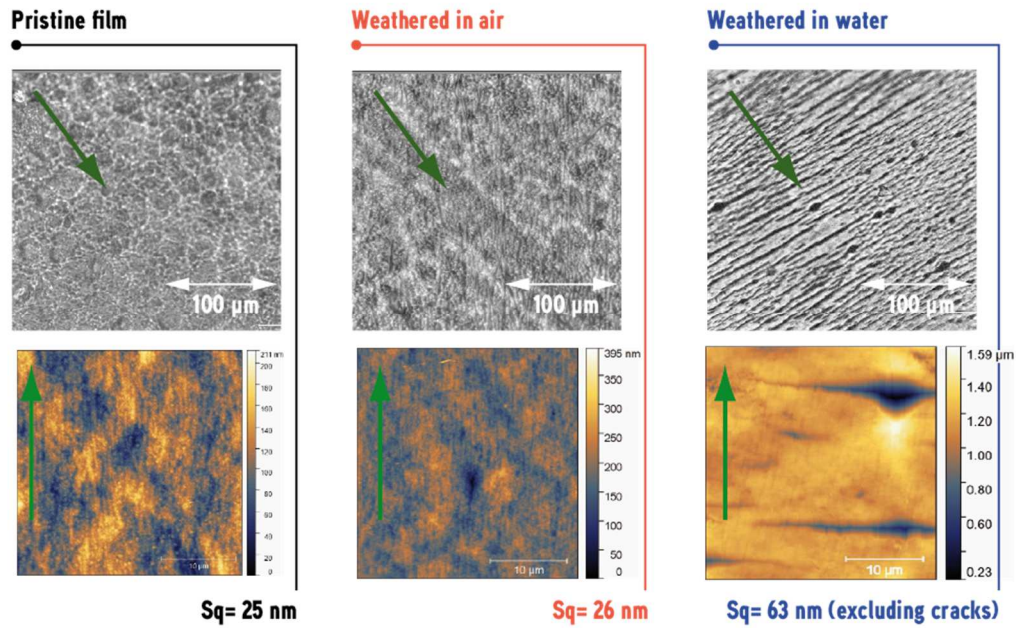
164 Figure 1: Photography between crossed polarizers of the pristine, air weathered and water weathered  
165 films after 25 weeks. Size distribution in abundance of fragments from samples weathered in water.

166

### 167 *Surface analysis*

168 In order to detect the presence of cracks on the film surfaces, their surface microstructures  
169 were studied by optical microscopy and Atomic Force Microscopy (Figure 2). Optical  
170 microscopy images indicate that macrocracks (defined here as cracks with length  $> 100\mu\text{m}$ )  
171 are only visible on the films weathered in water and that these cracks are oriented  
172 perpendicular to the extrusion direction. For air condition, the macroscopic structure of the  
173 film surfaces appear unchanged compared to pristine films.

174



175

176 Figure 2. Optical microscopy (800x600μm, top) and AFM topography (30x30μm, bottom) images of  
 177 the different films after 25 weeks. The green arrow represents the extrusion direction.

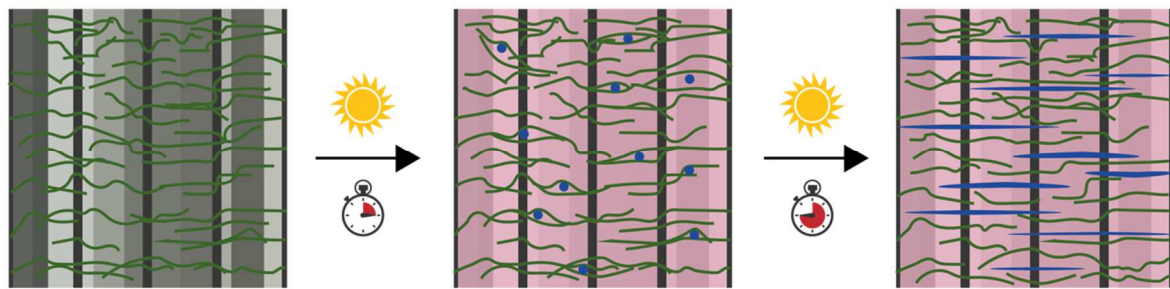
178

179 At a lower range, AFM topography images show that for all the films, micrometric lines in  
 180 parallel to the extrusion direction lines are visible. They represent the crystalline lamellae  
 181 alignment due to stress caused by the film formation process and are similar for all films  
 182 (Zhang et al. 2004). On the water-weathered films, microcracks (length <10μm) are visible  
 183 between the macrocracks, normally to the extrusion direction (Deblieck et al. 2011) whereas  
 184 no such defaults appear for the air condition. As already described in literature, the main  
 185 mechanism for the fracture development in a semi-crystalline polymer is initiated through the  
 186 formation of nano-cavities (voids) in the amorphous phase. It appears here that such voids in  
 187 the amorphous region led to microcracks only in the water condition together with an increase  
 188 of the surface roughness between the microcracks as indicated by the topography analysis (63  
 189 nm vs 26 nm). During weathering these voids can coalesce, leading eventually to the  
 190 formation of micro and macrocracks preferentially in the direction of the tie chains

191 (Zhang and Jar 2016). The propagation of the macrocracks along the direction normal to the  
192 extrusion direction lead to the fragmentation of the film in fragments with longitudinal shapes  
193 (Figure 1). These observations are schematized on Figure 3 which represents the structure of a  
194 blown-extruded film with the aligned crystalline phases (bold and black vertical lines) parallel  
195 to the extrusion direction. Polymer chains in the crystalline region extend into the amorphous  
196 regions as tie chains (green longitudinal lines). In the amorphous phase, voids are created and  
197 when weathering in water, they coalesce until the formation of macrocracks which will drive  
198 the shape of generated fragments.

199

200



201

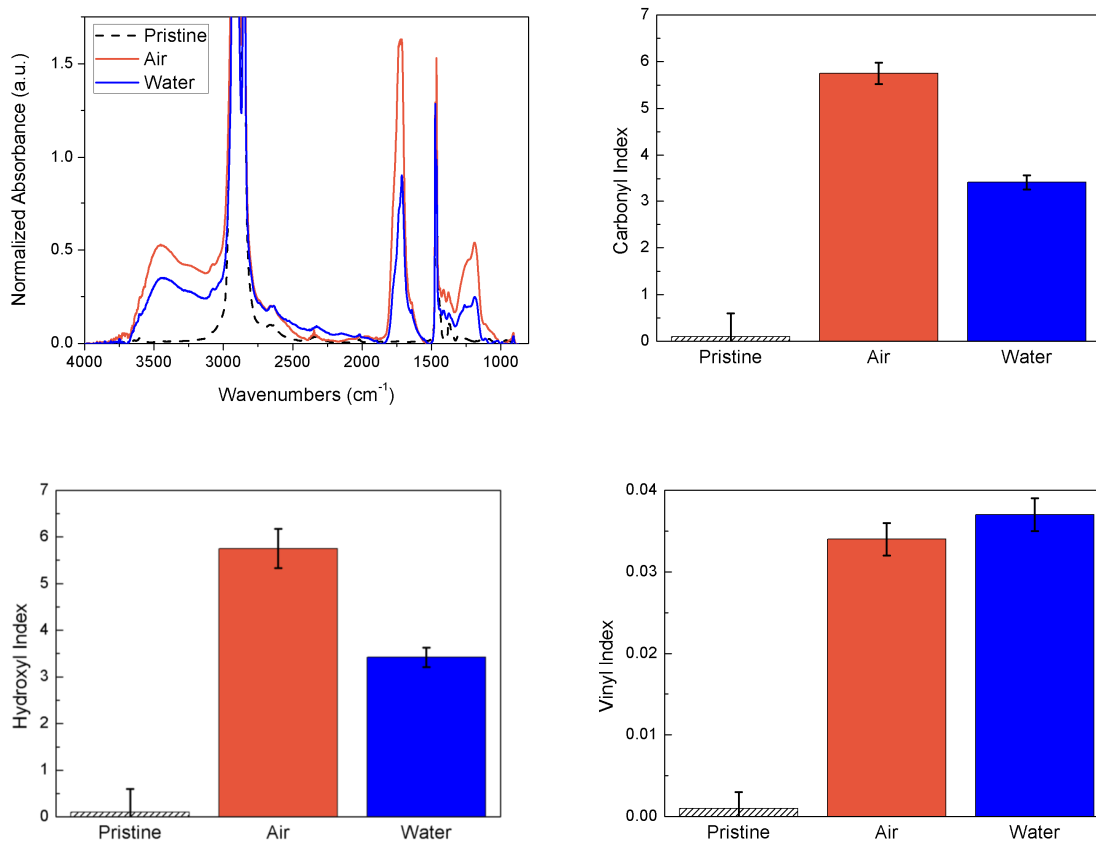
202 Figure 3. (a) Schematic structure of the blown-extruded LDPE films. The crystalline lamellae (bold  
203 straight lines) are aligned in parallel to the extrusion direction and perpendicularly to the amorphous  
204 phase (i.e. tie chains, light longitudinal lines). (b) Due to the weathering, crack initiation begin with  
205 the formation of void (blues circles), (c) in water, the coalescence of voids leads to the formation of  
206 micro- and macro-cracks (blues horizontals lines).

207

### 208 ***Oxidation monitoring***

209 Photodegradation leads to modification of the polymer chemistry through the introduction of  
210 various oxygenated moieties. These molecular changes conduct to competitive reactions of  
211 chain scission and crosslinking (Xiong et al. 2016). Chemical modification of the weathered

212 films were characterized by FTIR spectroscopy through the study of the variation of different  
 213 indexes namely carbonyl index (CI) for the apparition of C=O bonds; hydroxyl index (HI) for  
 214 O-H bonds and vinyl index (VI) for C=C bonds. Although, the definition of the frequency  
 215 range and the choice of the reference band can vary from one study to another, the evolution  
 216 of these indexes are good indicators of the evolution of the oxidative reactions (Andrady



217 2017; ter Halle et al. 2017).

218 Figure 4. FTIR normalized spectra and corresponding evolution of CI, HI and VI for the different  
 219 weathering conditions after 25 week of weathering

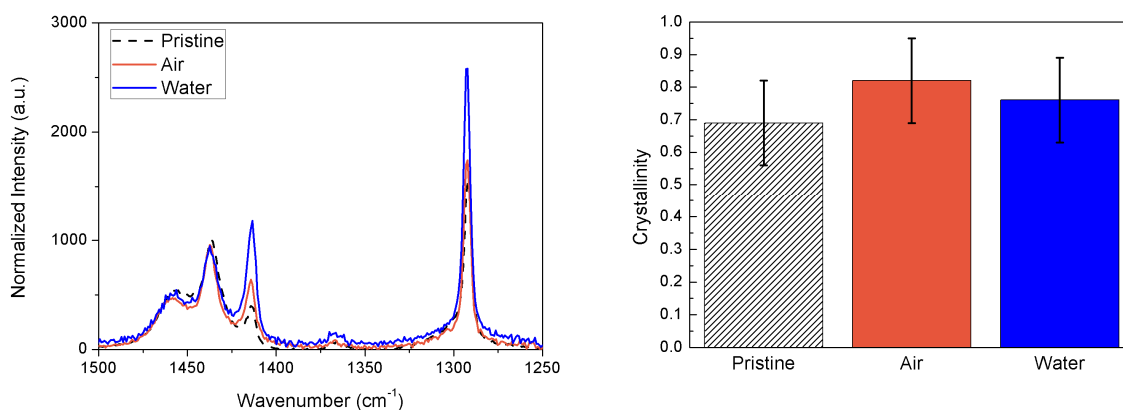
220

221 Figure 4 shows the normalized FTIR spectra of the different films and the evolution of the  
 222 different indexes after 25 week of weathering in air and water. It can be seen that  
 223 independently of the condition all indexes increased after weathering indicating a strong

224 chemical modification of the LDPE films. Whereas no clear difference is observed between  
225 air and water for the evolution of VI, weathering in air leads to higher CI and HI than  
226 weathering in water. Despite the presence of cracks in water-weathering films which is  
227 supposed to increase the exposed surface to light modification, these results indicate that a  
228 higher quantity of C=O and O-H bonds were produced on the LDPE surfaces during the  
229 weathering in air.

230

### 231 *Crystallinity*



232

233 Figure 5. Normalized (with 2720 cm<sup>-1</sup> band) confocal Raman spectra and corresponding evolution of  
234 crystallinity after 25 week of weathering.

235

236 In semi-crystalline polymers such as LDPE, oxidation mainly occurs in amorphous regions in  
237 which oxygen can readily diffuse. This oxidation process induces chain splits and accordingly  
238 low molecular weight free segments are formed. Due to their smaller size, they can rearrange  
239 into a crystalline phase leading to the process of chemi-crystallization which can be illustrated  
240 by an increase of the crystallization degree after weathering (Ojeda et al. 2011). In this study  
241 since some samples were fragmented, determination of the crystallinity using Differential  
242 Scanning Calorimetry (DSC) was not possible. Moreover since chemi-crystallization is a

243 surface phenomenon (Yakimets, Lai, and Guigon 2004), confocal Raman spectroscopy which  
244 is sensitive to the first micrometers of the film surfaces can be used (Delorme et al. 2003). To  
245 our knowledge no simple method based on Raman spectrometry is able to give quantitative  
246 crystallinity degree values. However, since crystalline and amorphous domains exhibit unique  
247 conformational characteristics, the frequency and bandwidth of the corresponding vibrational  
248 modes in Raman spectrum are different. The study of the relative evolution of these  
249 vibrational bands can give some qualitative information on the evolution of the crystallinity of  
250 the material. Figure 5 shows the evolution of the ratio of area integral Raman intensity  
251 between the 1416 cm<sup>-1</sup> band (CH<sub>2</sub> crystalline phase) and the reference 2720 cm<sup>-1</sup> band (CH  
252 stretching) for the different weathering conditions (Lin et al. 2007). Figure 5 indicates no  
253 clear increase of the surface crystallinity for the weathered samples compared to the pristine  
254 film.

### 255 *Mechanical properties*

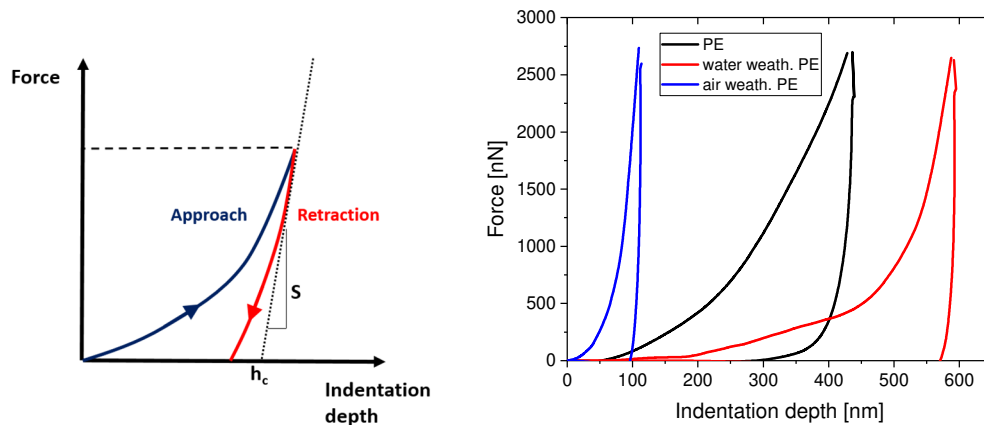
256 The mechanical properties of the film surfaces were studied by AFM. Indeed, AFM has the  
257 ability compared to classical mechanical tests (tensile tests, DMA...) to allow measurements  
258 of the elastic properties even on small fragments. The elastic modulus of the films can be  
259 calculated using the following equation (Schiffmann 2011):

260

$$261 \quad E = \frac{S\sqrt{\pi}}{2\sqrt{A} \times (1 - \nu^2)}$$

262

263 where S is the experimentally measured stiffness (Figure 6) of the very beginning region of  
264 the unloading curve, A is the projected area of contact between the indenter and the sample at  
265 the corresponding deformation, and  $\nu$  is the Poisson ration ( $\nu=0,4$  for LDPE) (Jee and Lee  
266 2010). The projected contact area A between the indenter and the sample was estimated from  
267 the surface area of the AFM tip which was determined by deconvolution (Ferencz et al. 2012).



269

270

271 Figure 6. a) Schematic force-indentation curve on polymer and corresponding characteristic  
 272 parameters b) Averaged force-indentation curves measured as function of the weathering conditions.

273

274

	S (N/m)	hc (nm)	A (m <sup>2</sup> )	E (GPa)
Pristine PE	339	430	4,54E-12	0,17
Air weathered	2549	112	3,06E-13	4,86
Water weathered	1975	592	8,60E-12	0,71

275 Table 1. Surface elastic moduli and corresponding experimental parameters extracted from the  
 276 averaged force indentation curves presented on Figure 6.

277

278

279 All results are summarized in Table 1. The film elastic modulus of pristine LDPE was found  
 280 to be 0,17 GPa which is in agreement with previous studies validating the measurement  
 281 procedure (Jee and Lee 2010). After 25 weeks of weathering, whatever the environment, a  
 282 hardening of the film surface (i.e. increase of the elastic modulus) can be observed but with

283 different magnitudes. The averaged elastic modulus increases by a factor of 30 for the films  
284 weathered in air and only by a factor of 4 for the film weathered in water.

285 The increase of the surface rigidity impacts the crack propagation process. Indeed assuming  
286 Irwin model (Yarema 1996), the critical stress for crack propagation can be expressed as:

$$287 \quad \sigma_{cr}^2 = G E / (\pi a)$$

288 where  $G$  is the total strain energy (plastic+elastic),  $2a$  is the length of the crack and  $E$  is the  
289 elastic modulus. Crack propagation only occurs when the released strain energy is greater  
290 than the energy required to create a fracture surface. The higher the Young modulus is, the  
291 higher will be the resistance to crack propagation (Deblieck et al. 2011).

292

293

#### 294 **Discussion: From oxidation to fragmentation**

295

296 All the results show that the presence of water influences clearly the fragmentation pathways  
297 of LDPE films. After a long weathering duration, a difference of surface oxidation was  
298 monitored between water and air conditions. The lowest oxidation observed on the films in  
299 water may be explained by a light exposure less important due to the light absorption by the  
300 water molecules. This was already described for polymers weathered in the natural  
301 environment (Andrady 1990; Brandon, Goldstein, and Ohman 2016). In this study, it is not  
302 the case because LDPE films (e.g. density=0.92) float on the water surface and the exposition  
303 intensity is the same than for sample weathered in air. The lower temperature of the film in  
304 water compared to the film in air may also explain the difference of oxidation since the  
305 temperature is known to accelerate the oxidation process (i.e. thermooxidation). However, in  
306 this experiment the temperature difference is rather low (59°C for air and 53°C for water).

307 Consequently, it is probable that the lower oxidation of the LDPE films in water observed  
308 here may be explained by the lower oxygen availability in water compared to air (Truesdale,  
309 Downing, and Lowden 2007). Because of the non-polar nature of LDPE and the absence of  
310 hetero-atoms, aging by hydrolysis was not considered (Gewert et al. 2015).

311

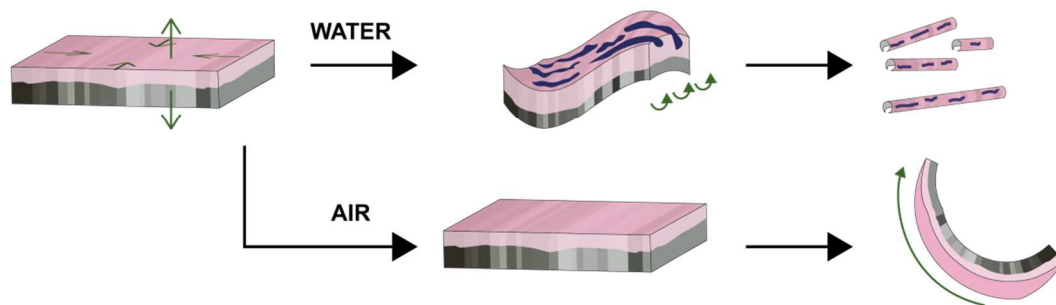
312 Oxidation promotes chain scissions in the amorphous phases, chains rearrangement (with  
313 increase of the crystallinity) and crosslinking between chains in the amorphous phase. It can  
314 be assumed that these changes result in an increase of the surface rigidity (Craig et al. 2005).  
315 Indeed, after a long weathering duration in the air, the films present a higher oxidation level  
316 and a higher crystallinity at their surface compared to water condition resulting in a high  
317 surface rigidity as demonstrated by AFM. For water condition, the oxidation and crystallinity  
318 degrees increased less than at air, leading to a lower surface rigidity. Besides, the huge  
319 difference in rigidity observed here can also be explained by the role of water as a plasticizer  
320 (Levine and Slade 1988). Actually, this effect consists in the penetration of small molecules  
321 between the polymer chain which prevents the rearrangements of polymer chains involved in  
322 crosslinking (Robeson 2013). All these chemical modifications - thickness of the crystalline  
323 lamellae, side chain concentration, fraction of ordered molecules in the crystalline regions,  
324 surface rigidity - appear first at the surface of the polymer. Yakimets et al. (2004)  
325 demonstrated that polymer films having undergone photodegradation are first altered in  
326 surface and no molecular chain scission appear in the core until the molar mass of the sample  
327 at the surface decreases considerably. This results in an incompatibility between tensile stress  
328 within the upper degraded layer (surface) and the compressive stress in the unchanged  
329 material layer. In addition together with manufacturing stress, these stresses cause the bending  
330 of the film along the extrusion direction (Choi et al. 2005) as shown in air condition (Figure  
331 1).

332

333 Moreover, the modification of surface rigidity clearly influences the resistance of the polymer  
334 to crack initiation (Barry and Delatycki 1992). According to Irwin model, the increase of the  
335 surface rigidity prevents the cracks propagation. The results presented here suggest that in air  
336 condition, the surface rigidity of the film is too high to allow crack initiation and propagation.  
337 An external stress is necessary to achieve fragmentation (Kalogerakis et al. 2017). On the  
338 contrary, the plasticizer effect of water may limit the increase of the rigidity of the film  
339 weathered in water, decreasing its resistance to crack initiation. Moreover, as a liquid, water  
340 governed by driving forces can transport through the craze fibril structure facilitating stress  
341 cracking as was already shown for liquids with high degree of absorption into a polymer  
342 (Robeson 2013). However to our knowledge and probably because of the lack of affinity of  
343 water toward polyethylene material, the ability of water to be a crack promoter for polyolefins  
344 has never been studied. Nevertheless, the oxidation of LDPE due to the weathering is going to  
345 increase the hydrophilicity of LDPE and increase the ability of water to act as a crack  
346 promoter. The enlargement of cracks lead to the fragmentation of the polymer in water  
347 without the necessity of any other external stress. In this case, the cracking propagation and  
348 the manufacturing process appear to be the major factor governing the initial shape of the  
349 fragments.

350 As a consequence, the fragments formed in water condition exhibited similar shapes and sizes  
351 at the millimetric scale. It appears that fragments with micrometric size ( $< 1$  mm) are not  
352 abundant as they represent only 10 % of the fragments. Surprisingly, the distribution  
353 presented here is close to the one reported for an extensive set of environmental samples  
354 (Cózar et al. 2014). In our case, it is a model study on PE under photodegradation in water in  
355 abiotic conditions. The degradation is strongly accelerated compared to environmental  
356 conditions where lower UV and temperature conjugated with the presence of biofilm at the

357 polymer surfaces are supposed to prevent the degradation (Rummel et al. 2017). It might then  
358 be supposed that in the real aquatic environment, the production of small microplastics  
359 through fragmentation processes would be a slow and difficult process compared to  
360 conditions of weathering at air and with the presence of a mechanical stress.  
361



362  
363 Figure 7. Sketch resuming the behavior of LDPE film in different weathering environments.

364  
365 **Conclusion**

366 This study confirms that the LDPE films weathering, either in water or at air, leads to the  
367 introduction of oxygenated groups, chain scission and rearrangement on the uppermost  
368 surface of the films. As observed for the air weathered films, above a threshold value the  
369 increase of surface hardening prevents the initiation of cracks because voids formation is  
370 limited. Since no cracks can be created and propagate, the induced stress can only be released  
371 through the wrapping of the film along the direction of the maximum stress which is in our  
372 case the extrusion direction as summarized in Figure 7. When a weak external stress is then  
373 imposed to the aged film, a catastrophic crack propagation is observed, which appears to be  
374 independent of the extrusion direction.

375 For the water-weathered films, the increase of surface rigidity due to crosslinking is not  
376 sufficient to prevent the initiation and propagation of cracks. As a consequence, the induced

377 stress can be release partly through crack propagation and partly through film wrapping as  
378 observed by the formation of wrapped fragments covered by macro and micro-cracks.  
379 Moreover, water probably accelerates the propagation of cracks: once the liquid penetrates to  
380 the craze tip, it then begins to plasticize the polymer and allows the craze to grow.

381 In both weathering conditions, the cracking of polymers did not appear correlated with the  
382 oxidation level. Indeed, despite a lower oxidation of plastics weathered in water as shown  
383 here and already described in literature for environmental weathering, the fragmentation may  
384 be faster in water than at air in the absence of mechanical stress. Moreover, this study shows  
385 that the mechanical properties at the film surface play a major role in the fragmentation  
386 pathway. The fabrication process is also important since for blown extruded LDPE the  
387 orientation of the polymer chains is going to influence the propagation direction of the cracks  
388 (i.e. normal to the extrusion direction). This preferential fracture direction may influence the  
389 size and shape distribution of the resulting fragments compared to air-weathered films.  
390 Consequently, the distribution of plastic fragments in the aquatic environment may be linked  
391 to the nature of the polymer but also to its manufacturing process. In this study, after 25  
392 weeks of weathering in water and high oxidation levels, 90 % of the fragments were > 1 mm  
393 in size with very similar shapes showing that micrometric fragments were not yet abundant.  
394 These results raise questions on the loss of fragments < 1 mm that was described in the  
395 environment. This loss may be due to the lack of methodology for sampling and analyzing  
396 small microplastics but also to the fact that long times of weathering and many steps of  
397 fragmentation appear necessary from macroplastics to reach sizes < 1 mm in water. These  
398 preliminary results have to be confirmed for other polymers and the long-term behavior of the  
399 so-generated fragments in water needs to be studied to predict their decrease in size among  
400 time. While a lot of studies show that the size of microplastics has a huge role on their  
401 impacts on marine life, only a little is known about the formation of microplastics and the

402 parameters that have effects on their size distribution. This work is among the first attempts to  
403 understand the pathways leading from macroplastics to microplastics.

404

405

#### 406 **Acknowledgements**

407 This work was funded by the French National Research Agency ANR through  
408 NANOPLASTICS (ANR-15-CE34-0006-02) and BASEMAN (ANR-15-JOCE-0001-01)  
409 projects. We also would like to thank Nadine Auriault and Roxane Noblat from CTTM  
410 (Centre de Transfert et Technologie du Mans) for their help with extrusion process and Cécile  
411 Brault for her help in figure drawing.

412

413

#### 414 **Bibliography**

415 Alkhadra, Mohammad A., Samuel E. Root, Kristan M. Hilby, Daniel Rodriguez, Fumitaka  
416 Sugiyama, and Darren J. Lipomi. 2017. "Quantifying the Fracture Behavior of Brittle  
417 and Ductile Thin Films of Semiconducting Polymers." *Chemistry of Materials*  
418 29(23):10139–49.

419 Andrady, Anthony L. 1990. "Weathering of Polyethylene (LDPE) and Enhanced  
420 Photodegradable Polyethylene in the Marine Environment." *Journal of Applied Polymer*  
421 *Science* 39(2):363–70.

422 Andrady, Anthony L. 2017. "The Plastic in Microplastics: A Review." *Marine Pollution*  
423 *Bulletin* 119(1):12–22file:///C:/Users/FABIEN~1/AppData/Local/Temp/.

424 Arthur, Courtney, Joel Baker, and Holly Bamford. 2009. "Proceedings of the International  
425 Research Workshop on the Occurrence, Effects, and Fate of Microplastic Marine  
426 Debris." *Group* (January):530.

427 Barnes, David K. A., Francois Galgani, Richard C. Thompson, and Morton Barlaz. 2009.  
428 “Accumulation and Fragmentation of Plastic Debris in Global Environments.”  
429 *Philosophical Transactions of the Royal Society B: Biological Sciences* 364(1526):1985–  
430 98.

431 Barry, D. B. and O. Delatycki. 1992. “The Effect of Molecular Structure and Polymer  
432 Morphology on the Fracture Resistance of High-Density Polyethylene.” *Polymer*  
433 33(6):1261–65.

434 Brandon, Jennifer, Miriam Goldstein, and Mark D. Ohman. 2016. “Long-Term Aging and  
435 Degradation of Microplastic Particles: Comparing in Situ Oceanic and Experimental  
436 Weathering Patterns.” *Marine Pollution Bulletin* 110(1):299–308.

437 Choi, Byoung-Ho, Alexander Chudnovsky, Rajesh Paradkar, William Michie, Zhenwen  
438 Zhou, and Pak-Meng Cham. 2009. “Experimental and Theoretical Investigation of Stress  
439 Corrosion Crack (SCC) Growth of Polyethylene Pipes.” *Polymer Degradation and*  
440 *Stability* 94(5):859–67.

441 Choi, Byoung-Ho, Zhenwen Zhou, Alexander Chudnovsky, Salvatore S. Stivala, Kalyan  
442 Sehanobish, and Clive P. Bosnyak. 2005. “Fracture Initiation Associated with Chemical  
443 Degradation: Observation and Modeling.” *International Journal of Solids and Structures*  
444 42(2):681–95.

445 Cózar, Andrés, Fidel Echevarría, J. Ignacio González-Gordillo, Xabier Irigoien, Bárbara  
446 Úbeda, Santiago Hernández-León, Álvaro T. Palma, Sandra Navarro, Juan García-de-  
447 Lomas, and Andrea Ruiz. 2014. “Plastic Debris in the Open Ocean.” *Proceedings of the*  
448 *National Academy of Sciences* 111(28):10239–44.

449 Craig, I. H., J. R. White, A. V. Shyichuk, and I. Syrotynska. 2005. “Photo-Induced Scission  
450 and Crosslinking in LDPE, LLDPE, and HDPE.” *Polymer Engineering & Science*  
451 45(4):579–87.

452 Deblieck, Rudy A. C., D. J. M. van Beek, Klaas Remerie, and Ian M. Ward. 2011. "Failure  
453 Mechanisms in Polyolefines: The Role of Crazing, Shear Yielding and the Entanglement  
454 Network." *Polymer* 52(14):2979–90.

455 Delorme, N., J. F. Bardeau, D. Nicolas-Debarnot, A. Bulou, and F. Poncin-Epaillard. 2003.  
456 "New Route for the Elaboration of Polyolefin Surfaces Bearing Azo Molecules."  
457 *Langmuir* 19(13):5318–22.

458 Ferencz, R., J. Sanchez, B. Blümich, and W. Herrmann. 2012. "AFM Nanoindentation to  
459 Determine Young's Modulus for Different EPDM Elastomers." *Polymer Testing*  
460 31(3):425–32.

461 Frank, A., G. Pinter, and R. W. Lang. 2009. "Prediction of the Remaining Lifetime of  
462 Polyethylene Pipes after up to 30 Years in Use." *Polymer Testing* 28(7):737–45.

463 Gewert, Berit, Merle M. Plassmann, and Matthew MacLeod. 2015. "Pathways for  
464 Degradation of Plastic Polymers Floating in the Marine Environment." *Environmental*  
465 *Science: Processes & Impacts* 17(9):1513–21.

466 Geyer, Roland, Jenna Jambeck, and Kara Law. 2017. "Production, Use, And Fate Of All  
467 Plastics Ever Made." *Science Advances* 3(7):25–29.

468 ter Halle, Alexandra, Lucie Ladirat, Marion Martignac, Anne Françoise Mingotaud, Olivier  
469 Boyron, and Emile Perez. 2017. "To What Extent Are Microplastics from the Open  
470 Ocean Weathered?" *Environmental Pollution* 227:167–74.

471 Jahnke, Annika, Hans Peter H. Arp, Beate I. Escher, Berit Gewert, Elena Gorokhova, Dana  
472 Kühnel, Martin Ogonowski, Annegret Potthoff, Christoph Rummel, Mechthild Schmitt-  
473 Jansen, Erik Toorman, and Matthew MacLeod. 2017. "Reducing Uncertainty and  
474 Confronting Ignorance about the Possible Impacts of Weathering Plastic in the Marine  
475 Environment." *Environmental Science & Technology Letters* 4(3):85–90.

476 Jee, Ah-Young and Minyung Lee. 2010. "Comparative Analysis on the Nanoindentation of

477 Polymers Using Atomic Force Microscopy.” *Polymer Testing* 29(1):95–99.

478 Kalogerakis, Nicolas, Katerina Karkanorachaki, G. Calypso Kalogerakis, Elisavet I.

479 Triantafyllidi, Alexandros D. Gotsis, Panagiotis Partsinevelos, and Fabio Fava. 2017.

480 “Microplastics Generation: Onset of Fragmentation of Polyethylene Films in Marine

481 Environment Mesocosms.” *Frontiers in Marine Science* 4(March):1–15.

482 Koelmans, Albert A., Merel Kooi, Kara Law, and Erik Van Sebille. 2017. “All Is Not Lost:

483 Fragmentation of Plastic at Sea.” *Environmental Science & Technology*

484 submitted(11):114028.

485 Levine, H. and L. Slade. 1988. “Water as a Plasticizer: Physico-Chemical Aspects of Low-

486 Moisture Polymeric Systems.” Pp. 79–185 in *Water Science Reviews 3: Water*

487 *Dynamics*, edited by Cambridge University Press: Cambridge.

488 Lin, W., M. Cossar, V. Dang, and J. Teh. 2007. “The Application of Raman Spectroscopy to

489 Three-Phase Characterization of Polyethylene Crystallinity.” *Polymer Testing*

490 26(6):814–21.

491 Ojeda, Telmo, Ana Freitas, Kátia Birck, Emilene Dalmolin, Rodrigo Jacques, Fátima Bento,

492 and Flávio Camargo. 2011. “Degradability of Linear Polyolefins under Natural

493 Weathering.” *Polymer Degradation and Stability* 96(4):703–7.

494 Phuong, Nam Ngoc, Aurore Zalouk-Vergnoux, Laurence Poirier, Abderrahmane Kamari,

495 Amélie Châtel, Catherine Mouneyrac, and Fabienne Lagarde. 2016. “Is There Any

496 Consistency between the Microplastics Found in the Field and Those Used in Laboratory

497 Experiments?” *Environmental Pollution* 211:111–23.

498 Robeson, Lloyd M. 2013. “Environmental Stress Cracking: A Review.” *Polymer Engineering*

499 *& Science* 53(3):453–67.

500 Rummel, Christoph D., Annika Jahnke, Elena Gorokhova, Dana Kühnel, and Mechthild

501 Schmitt-Jansen. 2017. “Impacts of Biofilm Formation on the Fate and Potential Effects

502 of Microplastic in the Aquatic Environment.” *Environmental Science & Technology*  
503 *Letters* 4(7):258–67.

504 Schiffmann, Kirsten Ingolf. 2011. “Determination of Fracture Toughness of Bulk Materials  
505 and Thin Films by Nanoindentation: Comparison of Different Models.” *Philosophical*  
506 *Magazine* 91(7–9):1163–78.

507 Šindelář, P., E. Nezbedová, P. Šimková, Z. Buráň, and P. Bohatý. 2005. “Effect of Structural  
508 Parameters on Rapid Crack Propagation and Slow Crack Growth in High Density  
509 Polyethylene Pipeline Materials.” *Plastics, Rubber and Composites* 34(7):329–33.

510 Truesdale, G. A., A. L. Downing, and G. F. Lowden. 2007. “The Solubility of Oxygen in Pure  
511 Water and Sea-Water.” *Journal of Applied Chemistry* 5(2):53–62.

512 Xiong, Jian, Kai Ni, Xia Liao, Jingjun Zhu, Zhu An, Qi Yang, Yajiang Huang, and Guangxian  
513 Li. 2016. “Investigation of Chemi-Crystallization and Free Volume Changes of High-  
514 Density Polyethylene Weathered in a Subtropical Humid Zone.” *Polymer International*  
515 65(12):1474–81.

516 Yakimets, Iryna, Dawei Lai, and Michèle Guigon. 2004. “Effect of Photo-Oxidation Cracks  
517 on Behaviour of Thick Polypropylene Samples.” *Polymer Degradation and Stability*  
518 86(1):59–67.

519 Yarema, S. Ya. 1996. “On the Contribution of G. R. Irwin to Fracture Mechanics.” *Materials*  
520 *Science* 31(5):617–23.

521 Zhang, X. ..., S. Elkoun, A. Ajji, and M. .. Huneault. 2004. “Oriented Structure and Anisotropy  
522 Properties of Polymer Blown Films: HDPE, LLDPE and LDPE.” *Polymer* 45(1):217–29.

523 Zhang, Yi and P. Y. Ben Jar. 2016. “Characterization of Damage Developm Ent in Semi-  
524 Crystalline Polymers.” Pp. 121–30 in *Polymer science: research advances, practical*  
525 *applications and educational aspects*, edited by E. A. Méndez-Vilas; A. Solano.  
526 Formatex Research Center.